ARTICLE
Journal of Cellular Biochemistry 112:307–317 (2011)

Journal of Cellular Biochemistry

Cell-Cycle-Dependent Localization of Human Cytomegalovirus UL83 Phosphoprotein in the Nucleolus and Modulation of Viral Gene Expression in Human Embryo Fibroblasts In Vitro

Maria-Cristina Arcangeletti,[1*] Isabella Rodighiero,[1] Prisco Mirandola,[2] Flora De Conto,[1] Silvia Covan,[1] Diego Germini,[1] Sergey Razin,[3] Giuseppe Dettori,[1] and Carlo Chezzi[1]

[1] *Microbiology Section, Department of Pathology and Laboratory Medicine, University of Parma, Parma, Italy*

[2] *Section of Human Anatomy, Department of Anatomy, Pharmacology and Forensic Medicine, University of Parma, Parma, Italy*

[3] *Institute of Gene Biology, Russian Academy of Science, Moscow, Russia*

ABSTRACT

The nucleolus is a multifunctional nuclear compartment widely known to be involved in several cellular processes, including mRNA maturation and shuttling to cytoplasmic sites, control of the cell cycle, cell proliferation, and apoptosis; thus, it is logical that many viruses, including herpesvirus, target the nucleolus in order to exploit at least one of the above-mentioned functions. Recent studies from our group demonstrated the early accumulation of the incoming ppUL83 (pp65), the major tegument protein of human cytomegalovirus (HCMV), in the nucleolus. The obtained results also suggested that a functional relationship might exist between the nucleolar localization of pp65, rRNA synthesis, and the development of the lytic program of viral gene expression. Here we present new data which support the hypothesis of a potentially relevant role of HCMV pp65 and its nucleolar localization for the control of the cell cycle by HCMV (arrest of cell proliferation in G1–G1/S), and for the promotion of viral infection. We demonstrated that, although the incoming pp65 amount in the infected cells appears to be constant irrespective of the cell-cycle phase, its nucleolar accumulation is prominent in G1 and G1/S, but very poor in S or G2/M. This correlates with the observation that only cells in G1 and G1/S support an efficient development of the HCMV lytic cycle. We propose that HCMV pp65 might be involved in regulatory/signaling pathways related to nucleolar functions, such as the cell-cycle control. Co-immunoprecipitation experiments have permitted to identify nucleolin as one of the nucleolar partners of pp65. J. Cell. Biochem. 112: 307–317, 2011.

KEY WORDS: HCMV; NUCLEOLUS; ppUL83; IE GENES; CELL CYCLE

Human cytomegalovirus (HCMV) is a betaherpesvirus that replicates productively in many cell types in vivo and can persist throughout the lifetime of the host, following lytic infection. It is a widespread human pathogen that latently infects 50–90% of the world's population. Although primary infection of healthy individuals is usually asymptomatic, it can cause severe and even fatal diseases in immunocompromised patients, mostly following the reactivation of endogenous virus, and it is also responsible for birth defects as a consequence of congenital infection. To date, many questions related to the activation of the lytic program of HCMV in a variety of cell types, ranging from actively proliferating to terminally differentiated cells, and the mechanisms underlying these events remain to be fully elucidated.

Most of the studies aimed at shedding light on the above problems have been focused on the cellular functional domains that could be co-opted by the virus and are important for its replication. In this regard, the cell nucleus represents the site of replication and virus assembly for most of DNA viruses, including HCMV. It is becoming increasingly evident that the compartmentalization of the nucleus in functional domains is a dynamic and very effective

Grant sponsor: Scientific Research Funds of the University of Parma; Grant number: FIL 2008, FIL 2009.

*Correspondence to: Prof. Maria-Cristina Arcangeletti, Microbiology Section, Department of Pathology and Laboratory Medicine, University of Parma, Via A. Gramsci, 14, 43126 Parma, Italy.
E-mail: mariacristina.arcangeletti@unipr.it

Received 21 July 2010; Accepted 13 October 2010 • DOI 10.1002/jcb.22928 • © 2010 Wiley-Liss, Inc.
Published online 4 November 2010 in Wiley Online Library (wileyonlinelibrary.com).

condition allowing crucial events, like DNA replication, transcription, RNA processing and transport to the cytoplasm, to take place. To this end it is worth mentioning that many viruses are able to exploit this functional organization [Ishov et al., 2002; Arcangeletti et al., 2003; Boyne and Whitehouse, 2006; Michienzi et al., 2006; Shimakami et al., 2006; Callé et al., 2008].

One of the most important functional compartments of the nucleus is the nucleolus, a plurifunctional domain operating first of all as a ''ribosome-producing factory'' of the cell, but also involved in the maturation of certain non-ribosomal RNAs, as well as in the control of cell cycle, proliferation, and apoptosis [Pederson and Tsai, 2009]. Previous studies support the important role of nucleolus in DNA and RNA virus replication [Matthews, 2000; Boyne and Whitehouse, 2006; Michienzi et al., 2006; Shimakami et al., 2006; Callé et al., 2008; Greco, 2009]. Concerning HCMV, the association of specific viral components with different nuclear domains has been demonstrated [Sanchez et al., 1998; Ahn and Hawyard, 2000; Lee et al., 2004; Lymberopoulos and Pearson, 2007; Salsman et al., 2008]. In particular, our group has described accumulation in nucleoli of the major tegument protein pp65 of the incoming HCMV at very early stages of infection, also showing that a functional relationship is likely to exist between the nucleolar localization of pp65 and the correct development of HCMV lytic cycle [Arcangeletti et al., 2003, 2009]. In this respect, it is of importance that the nucleolus is involved in the control of the cell cycle in mammalian cells [Boisvert et al., 2007] also through its role in the biogenesis of ribosomes [Ruggero and Pandolfi, 2003; Pliss et al., 2005]. In particular, during G1, an increase in rRNA synthesis and ribosome assembly is necessary to satisfy the increased need for newly synthesized proteins at the beginning of the S phase. Nucleolar components control the above-mentioned processes, mostly by modulating the phosphorylation levels of transcription factors [Grinstein et al., 2006] that can influence their interaction with RNA polymerase I transcription machinery and its subsequent activation [Russell and Zomerdijk, 2005].

Targeting the nucleolus in order to take over control of the cell cycle may represent an important strategy for many viruses, crucial for the infection outcome [Dittmer and Mocarsky, 1997; Fortunato et al., 2002; Hiscox, 2002, 2007; Bain and Sinclair, 2007; Cawood et al., 2007; Galati and Bocchino, 2007; Sarfraz et al., 2008; Chang et al., 2009; Hamid et al., 2009].

It is possible that the nucleolar accumulation of the incoming HCMV pp65, with a postulated kinase activity [Somogyi et al., 1990], represents an important tool used by the virus in order to take over cellular regulatory systems, to control the progression of the cell cycle and to ensure the correct development of the lytic program.

The aim of the present study was to find out whether a relationship exists between the nucleolar localization of pp65, the cell-cycle stages and the efficiency of virus infection, by analyzing synchronous and asynchronous human fibroblasts in vitro using a fluorescence-activated cell sorter (FACS), immunofluorescence (IF), molecular and biochemical approaches. We demonstrate that, although virus entry (monitored by the incoming pp65 amount) appears to be constant, irrespective of the cell-cycle phase, the nucleolar accumulation of pp65 is prominent only in G1 and G1/S, while it is very poor in S and G2/M. It is also noteworthy that only the former phases seem to support an efficient development of the lytic infection and that the cell cycle is arrested in G1–G1/S in infected fibroblasts.

MATERIALS AND METHODS

CELL CULTURE

Monolayer cultures of MRC5 human embryo lung fibroblasts (American Type Culture Collection, ATCC; CCL-171) were grown in Earle's modified Minimum Essential Medium (E-MEM), supplemented with 2 mM L-glutamine, 1% non-essential aminoacids, 1 mM sodium pyruvate, 10% fetal bovine serum (FBS), and antibiotics (100 U/ml penicillin, 100 μg/ml streptomycin). Cell culture medium and supplements were from PAA (The Cell Culture Company).

VIRUS INFECTION AND TITRATION

The reference AD169 strain (ATCC VR-538) of HCMV was used for the in vitro infection of MRC5 fibroblasts. Viral infectious titer was determined by plaque assay, as already described [Arcangeletti et al., 2003]. All the experiments were performed using a multiplicity of infection (m.o.i.) of three plaque forming units (PFU)/cell.

VIRUS INACTIVATION

An aliquot of purified and titrated HCMV suspension was diluted in 1 ml of E-MEM without FBS and placed in a 3-cm Petri dish. Then it was irradiated for 2 h on ice, at a distance of 5 cm from an UV lamp. The UV-inactivated virus did not replicate, nor did it produce any detectable levels of immediate early (IE) gene products (data not shown).

ANTIBODIES

A purified monoclonal blend (clones 1C3 and AYM-1) reacting with the 65–68 kDa lower matrix structural phosphoprotein (pp65) of HCMV and a monoclonal antibody (Mab clone E13) specific for the common epitope encoded by exon 2 of the IE major products (72 and 86 kDa proteins) (Argene) were used for IF experiments [1:30 dilution in 0.2% bovine serum albumin (BSA) in phosphate-buffered saline (PBS: 7 mM Na_2HPO_4, 1.5 mM KH_2PO_4, pH 7.4, 137 mM NaCl, 2.7 mM KCl)]. Another monoclonal antibody raised against HCMV pp65 (clone 1-L-11, Santa Cruz, distributed by Tebu-bio; 1:200 dilution) was used for Western blotting (WB) analysis. An anti-tubulin monoclonal antibody (Abcam) and a rabbit polyclonal antibody to EAAT3 (EAAC1: excitatory amino acid carrier 1) (Santa Cruz) were employed as cytoplasmic markers (working dilutions: 1:200 and 1:500, respectively). A rabbit polyclonal antibody raised against an internal region of promyelocytic leukemia protein (PML) (Santa Cruz) was used to check the nucleoplasmic protein fractions purity (working dilution: 1:300). A series of polyclonal antibodies were used to detect nucleolar proteins: the ''ANA-N'' serum, a human anti-serum directed against a pool of nucleolar antigens (The Binding Site; undiluted) and a monospecific rabbit polyclonal antibody to nucleolin (C23) (Santa Cruz; working dilution: 1:200). Tetramethyl-rhodamine-isothiocyanate (TRITC)-conjugated goat anti-mouse IgG or Alexa-Fluor fluorescein

isothiocyanate (FITC)-conjugated goat anti-mouse IgG (H + L) (Molecular Probes), were used to detect viral antigens; Alexa-Fluor FITC-conjugated goat anti-human IgG (H + L) (Molecular Probes) was employed to reveal the nucleolar proteins pool. For WB analysis, anti-mouse- and anti-rabbit-alkaline phosphatase (AP)-conjugated antibodies (DakoCytomation) were used.

INDIRECT IMMUNOFLUORESCENCE

MRC5 cells were gently rinsed with cytoskeleton (CSK) buffer [10 mM pipes (1.4-piperazinediethanesulfonic acid), pH 6.9, 100 mM NaCl, 1.5 mM $MgCl_2$, 300 mM sucrose], simultaneously fixed and permeabilized with 2.5% Triton X-100 and 1% paraformaldehyde in CSK buffer at room temperature for 20 min [Arcangeletti et al., 1997], and then stained as previously described [Arcangeletti et al., 2003]. Finally, the cells were mounted with Prolong Gold anti-fade reagent (Molecular Probes) and analyzed by a fluorescence microscope (Leica DMLB).

CELL SYNCHRONIZATION

Cells were grown to confluence and maintained at high density in 75 cm^2 flasks in E-MEM supplemented with 10% FBS, then trypsinized, re-seeded at a density of 6×10^5 per 3-cm Petri dish, and allowed to grow for the indicated time points (see Fig. 1), before cellular DNA staining and flow cytometry analysis.

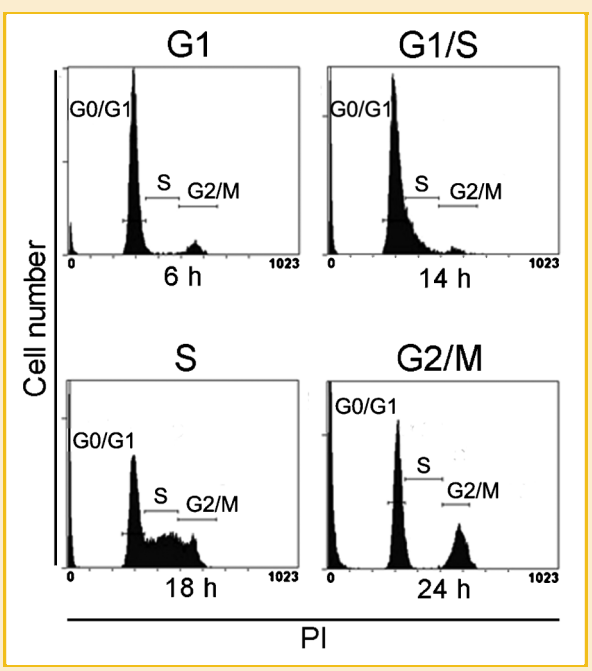

Fig. 1. Histogram of DNA content (propidium iodide, PI) versus number of cell counts (cell number), obtained by flow cytometry. MRC5 human embryo fibroblasts were grown to confluence and maintained at high density, then they were trypsinized and re-seeded in 3-cm Petri dishes for the indicated times (6, 14, 18, and, 24 h). Cells were harvested and stained with PI and their DNA content was analyzed by FACS.

INDIRECT IMMUNOFLUORESCENCE FOR FLOW CYTOMETRY ANALYSIS

After synchronization, cells were trypsinized, harvested, and centrifuged at 800*g* for 10 min at room temperature. The supernatant was discarded, the pellet resuspended in 0.6 ml of PBS and 1.4 ml of ethanol 100% (70% ice-cold ethanol) dropwise, and fixed/permeabilized overnight at −20°C. Then, cells were centrifuged at 800*g* for 10 min at room temperature, the supernatant was discarded and the pellet resuspended in 0.5 ml of PBS. The cells were pelleted again and stained for 30 min at room temperature in the dark using a mixture of primary antibodies in dilution buffer (0.5% BSA and 0.5% Tween-20 PBS). Then, cells were rinsed in wash buffer (0.5% BSA–PBS) and centrifuged; the pellet was resuspended in the appropriate dilution of Alexa-Fluor FITC-conjugated goat anti-mouse IgG secondary antibody and incubated for 30 min at room temperature in the dark. Cells rinsed in wash buffer were pelleted and resuspended in PBS containing propidium iodide (PI; 10 μg/ml) and RNase (100 μg/ml) and incubated for 30 min at room temperature. Control cells were stained with a monoclonal anti-rat IgG1-K (AbD Serotec).

FLOW CYTOMETRY

The samples prepared as described above were analyzed by the EPICS® XL-MCL cytometer (Beckman Coulter). DNA content and viral parameters in the different cell-cycle phases were analyzed by using the Expo32 Software (Beckman Coulter). Corresponding peaks of G0/G1, S, and G2/M were obtained excluding doublets and cell debris by FL3lin/RATIO and FS/FL3log dot-plot analysis, respectively [Gobbi et al., 2009]. Percentages shown in Figures 2, 4, and 5 were calculated from the raw data, obtained analyzing more than 10,000 events.

RNA ISOLATION AND RT-PCR ASSAY

Total RNA from infected MRC5 cells enriched in different cell-cycle phases [G1 and S; 3 and 24 h post-infection (p.i.)], was extracted according to the manufacturer's instructions (Macherey-Nagel, NucleoSpin® RNAII). Integrity of RNA was examined by denaturing agarose gel electrophoresis and sample quality and quantity were estimated measuring its adsorbance at 260 and 280 nm (Eppendorf–BioPhotometer). Then, according to SuperScript III One Step RT-PCR with Platinum *Taq* (Invitrogen) protocol, the template RNAs were reverse transcribed and subjected to PCR amplification using specific primers for IE1 (immediate-early), UL54 (DNA polymerase, early), UL83 (pp65, early-late), and UL32 (pp150, late) HCMV genes [Ioudinkova et al., 2006]. A GAPDH fragment of 257 bp was amplified as a control.

SUBCELLULAR FRACTIONATION

At the indicated time points after infection, the cell medium was removed and synchronized cells (G1 and S) were washed with cold PBS, and then trypsinized. According to Muramatsu and co-workers [Muramatsu et al., 1963; Muramatsu and Onishi, 1978], the pellet was washed with ice-cold PBS at 500*g* at 4°C. Then, cells were resuspended in 15 volumes of a buffer containing 10 mM Tris–HCl, pH 7.4, 10 mM NaCl, 1 mM $MgCl_2$ and incubated on ice for 30 min. Cells lysis was performed by addition of a final

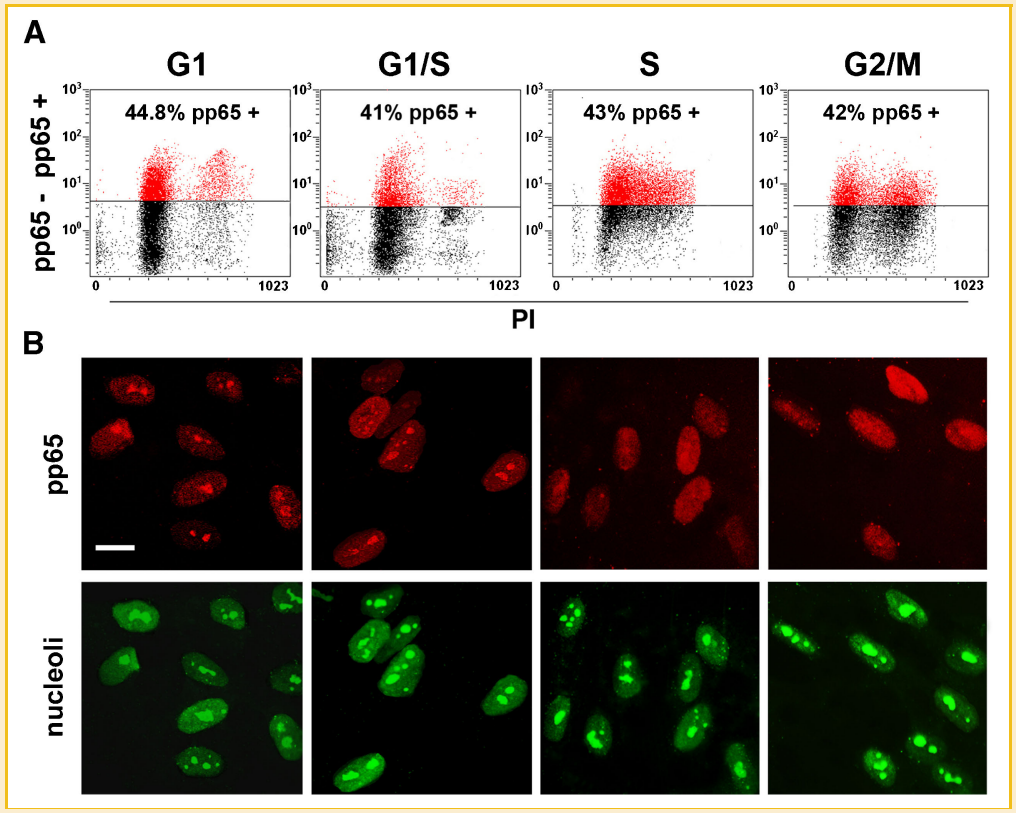

Fig. 2. Cellular distribution of HCMV pp65 of the parental virus in different phases of the cell cycle of synchronous MRC5 cells. Confluent monolayers of MRC5 fibroblasts (G0 phase) were subcultured for the time periods necessary to synchronize them in the indicated phases of the cell cycle, and then infected with HCMV AD169 (m.o.i. = 3; 3 h p.i.). Panel A: Flow cytometry analysis (dot-plot representation) of the tegument protein pp65 of the incoming virus and DNA content (propidium iodide, PI). Cells were stained with a monoclonal antibody against the 65–68 kDa HCMV lower matrix structural phosphoprotein; the immunoreaction was revealed using Alexa-Fluor FITC-conjugated goat anti-mouse IgG. Cells were also treated with PI to stain DNA, as detailed in the Materials and Methods section. Arbitrary colors were used in the graphics: infected cells (pp65+) are represented in red, while the uninfected cells (pp65−) are in black. The relative percentage of infected cells in different stages of the cell cycle is shown in the graphs. Panel B: Double-stain immunofluorescence microscopy analysis of the nuclear and nucleolar patterns of pp65 viral antigen and nucleolar proteins. MRC5 fibroblasts were grown on coverslips and infected with HCMV. Then cells were fixed and simultaneously labeled with a monoclonal antibody reacting with pp65 and a human anti-serum raised against a nucleolar antigen pool. The anti-pp65 antibody was revealed by Alexa-Fluor TRITC-conjugated goat anti-mouse IgG and nucleolar proteins were stained by Alexa-Fluor FITC-conjugated goat anti-human IgG. Images were collected using a conventional fluorescence microscope. Bar = 10 μm.

concentration of 0.3% Nonidet P-40 and homogenization was performed using a Dounce homogenizer. Nuclei were collected by centrifugation at 1,200*g* for 5 min. The supernatant, corresponding to the cytoplasmic fraction, was harvested and stored at −20°C for further analyses. Nuclei were resuspended in isotonic buffer (0.25 M sucrose, 10 mM $MgCl_2$), purified by centrifugation at 1,200*g* for 10 min through a 0.88 M sucrose cushion containing 0.05 mM $MgCl_2$, then resuspended in 10 volumes of 0.34 mM sucrose containing 0.05 mM $MgCl_2$. Nucleoli were purified from the above fraction by sonication (Sonoplus, Bandelin) on ice for several bursts of 30 s (5 min intervals between each run), then isolated from the resulting homogenate by centrifugation at 2,000*g* for 20 min through a 0.88 M sucrose cushion containing 0.05 mM $MgCl_2$. The supernatant, representing the nucleoplasmic fraction, as well as the resulting nucleolar pellet (resuspended in 0.34 M sucrose, 0.05 mM $MgCl_2$) were harvested and stored at −20°C for further analyses. Chemicals were from Sigma–Aldrich. Each cellular fraction was subjected to protein quantitation (Bradford method).

WESTERN BLOTTING ANALYSIS

After SDS-polyacrylamide gel electrophoresis (SDS-PAGE), proteins were transferred onto 0.45-μm pore-size nitrocellulose membranes (Bio-Rad) overnight at 4°C. Membranes were incubated for 2 h at room temperature in PBS supplemented with 0.2% Tween-20 (Sigma–Aldrich) and 4% non-fat dry milk and then for further 60 min, using the antibodies mentioned in the corresponding section. After several 5-min washes with PBS, membranes were incubated with anti-rabbit or anti-mouse AP-conjugated antibodies for 60 min at room temperature. Then, membranes were washed as described above, and the immunoreaction was visualized using Sigma Fast BCIP/NBT-buffered substrate. Molecular weight markers were from Bio-Rad (Fig. 3) and Fermentas (Fig. 6).

PROTEIN Co-IMMUNOPRECIPITATION (Co-IP)

Uninfected or infected cell monolayers were trypsinized, harvested in PBS and subjected to cell lysis, as described above. Cellular lysates were analyzed by co-immunoprecipitation (Co-IP) followed by WB

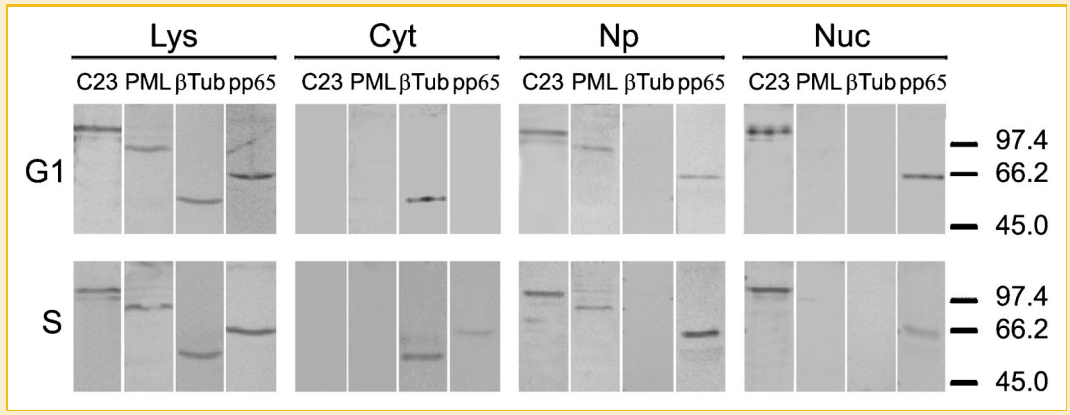

Fig. 3. Biochemical analysis of the cellular distribution of the viral pp65 versus nucleolar, nucleoplasmic, and cytoplasmic markers in different phases of the cell cycle of synchronous MRC5 cells. Confluent MRC5 monolayers (G0 phase) were subcultured for the time periods necessary to synchronize them in G1 and S phases, and then infected with HCMV AD169 (m.o.i. = 3; 3 h p.i.). Cells were then subjected to cellular fractionation, in order to obtain purified nucleoli (Nuc), nucleoplasm (Np), and cytoplasmic (Cyt) fractions, as well as the total cell lysate (Lys). Subsequently, SDS–PAGE and WB were done, using a monoclonal antibody directed to pp65, a monospecific polyclonal antibody raised against C23 (nucleolin), a monospecific polyclonal antibody against promyelocytic leukemia protein (PML) and a monoclonal antibody to β-tubulin as nucleolar, nucleoplasmic, and cytoplasmic fractionation markers, respectively. The immunoreactions were revealed by donkey anti-mouse-AP (pp65 and β-tubulin) and donkey anti-rabbit-AP (C23, PML) antibodies. Molecular weight markers are indicated on the right.

according to the manufacturer's instructions (ExactaCruz™ B or ExactaCruz™ C, Santa Cruz–Tebu-bio); this method improves the effectiveness of the immunoprecipitated proteins revealed by WB, eliminating the detection of heavy and light chains of the IP antibody. Briefly, 50 µl of suspended (25%, v/v) IP matrix (containing protein A/G PLUS-agarose), 5 µg of IP antibody (either a rabbit anti-nucleolin antibody or a mouse monoclonal anti-pp65 antibody; a pre-immune rabbit serum was used as IP negative control) and 500 µl of PBS were added to a microcentrifuge tube, mixed and incubated overnight at 4°C. Then, the IP antibody/IP matrix complex was pelleted in a microcentrifuge at maximum speed for 30 s at 4°C and the supernatant carefully discarded. The pelleted complex was washed two times with 500 µl of PBS; then, the cell lysate was transferred to the pelleted matrix and incubated overnight at 4°C. After incubation, it was microcentrifuged at maximum speed for 30 s at 4°C, and the pellet was washed four times with PBS. Finally, the pellet was resuspended in 50 µl of Laemmli buffer at 95°C for 5 min and centrifuged again as described above; then, the supernatant was loaded on a 12.5% SDS–polyacrylamide gel and transferred onto nitrocellulose membranes for WB, using the appropriate primary and secondary antibodies.

RESULTS

ANALYSIS OF CELLULAR LOCALIZATION OF THE INCOMING HCMV ppUL83 (pp65) IN DIFFERENT PHASES OF THE CELL CYCLE IN MRC5 SYNCHRONIZED CELLS

A cell synchronization protocol [Fortunato et al., 2002] was adapted to MRC5 cells cultivated to confluence (i.e., arrested in G0 by contact inhibition), trypsinized, re-seeded and allowed to grow for 6, 14, 18, and 24 h to have cells enriched in G1, G1/S, S, and G2/M, respectively, as shown in Figure 1.

In the next series of experiments, synchronized MRC5 cells were infected with the HCMV AD169 strain for 3 h. Analysis of the DNA content and distribution of HCMV pp65, representing the incoming virus entry, were carried out by flow cytometry (Fig. 2A). It appears evident that the amount of pp65 carried to cells as a result of infection is quite the same, irrespective of the cell-cycle phase, as shown by the percentage values on the dot-plot graphics (red spots: infected cells; black spots: uninfected cells). Thus, it seems that the ability of the virus to enter the cells is independent of the phase of the cell cycle.

At the same time the nuclear distribution of the pp65 turned out to be drastically different at the considered phases of the cell cycle (Fig. 2B). In this experiment, MRC5 fibroblasts enriched in G1, G1/S, S, and G2/M were infected with HCMV for 3 h and then double-labeled (nucleolar proteins: green; pp65: red) by indirect IF. The expected accumulation of pp65 within the nucleolar compartment [Arcangeletti et al., 2003, 2009] was only evident in G1- and G1/S-synchronized cells, while this pattern was either faintly observable in some cells (most likely cells still residing in G1) or absent in S and G2/M, where the viral protein was almost evenly distributed over the whole nucleus. It should be recalled that pp65 belongs to the "early-late" group of HCMV-encoded proteins; the expression of this protein does not start at 3 h p.i. Thus, the cellular distribution of pp65 described above did not include the viral protein synthesized in the cell, rather that present in virions and carried into cells upon infection.

In order to verify the conclusions based on flow cytometry and immunostaining results, we have analyzed the distribution of pp65 in subcellular fractions (in particular, between nucleolus and nucleoplasm) by WB. MRC5 cells were enriched in G1 and S phases and then infected with HCMV for 3 h. After infection, cell monolayers were harvested and subjected to cellular fractionation. Purified nucleoli (Nuc), nucleoplasmic (Np), and cytoplasmic (Cyt) fractions, as well as total lysate (Lys), were analyzed by SDS–PAGE and WB (Fig. 3), using an anti-pp65 antibody and antibodies against nucleolin (C23), PML, and tubulin (βTub) as nucleolar, nucleoplas-

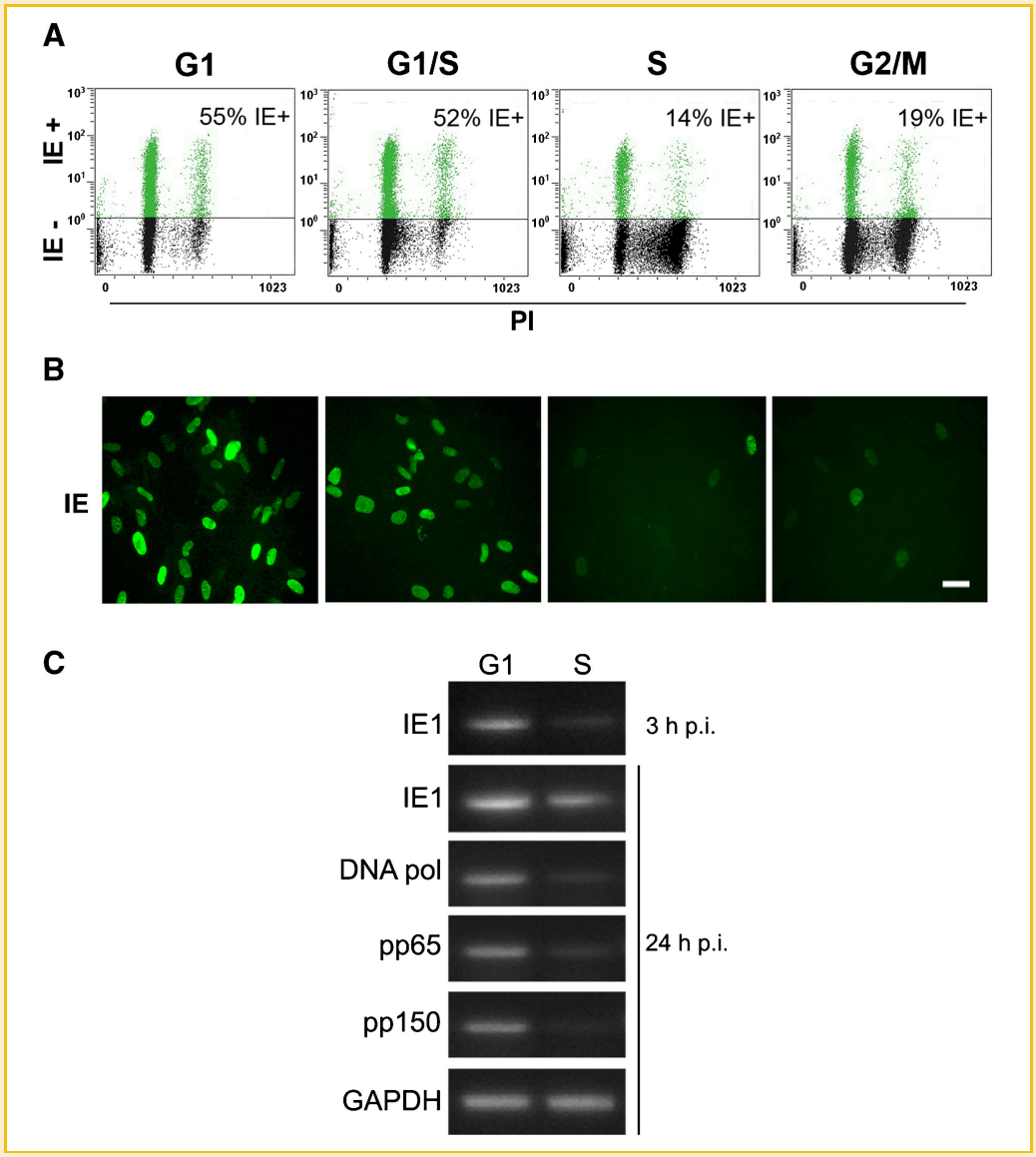

Fig. 4. HCMV immediate-early gene expression in different phases of the cell cycle of synchronous MRC5 cells. Confluent monolayers of MRC5 fibroblasts were subcultured for the time periods necessary to synchronize them in the indicated phases of the cell cycle, and then infected with HCMV AD169 (m.o.i. = 3). Panel A: Flow cytometry analysis (dot-plot representation) of the IE proteins and DNA content (propidium iodide, PI) in synchronized cells infected with HCMV for 3 h. Green dots indicate cells positive for viral immediate-early proteins (IE+); black dots represent uninfected cells (IE−). Panel B: Immunofluorescence microscopy analysis of HCMV IE antigens in synchronous MRC5 fibroblasts grown on coverslips and infected with HCMV for 3 h. Cells were fixed and labeled with the same monoclonal antibody reacting with IE used in A. The anti-IE antibody was revealed by Alexa-Fluor FITC-conjugated goat anti-mouse IgG. Images were collected using a conventional fluorescence microscopy. Bar = 20 μm. Panel C: RT-PCR amplification patterns of immediate-early, early, and late transcripts of HCMV in synchronous MRC5 cells. MRC5 fibroblast monolayers were subcultured for the time periods necessary to synchronize them in G1 and S phases and then infected with the HCMV. Total RNA was extracted at 3 or 24 h p.i. Viral transcripts were: IE1 (product length: 303 bp), DNA polymerase ("DNA pol" 237 bp), pp65 (213 bp), and pp150 (206 bp). GAPDH transcript was used as a control.

mic, and cytoplasmic markers, respectively. As expected (see Fig. 2A), the amount of pp65 in the total lysates from cells in G1 and S was almost equivalent. Furthermore, the results show that the distribution of pp65 in the considered cellular fractions varies depending on the cell-cycle phase. In particular, in G1 cells pp65 immunolabeling was very evident in the Nuc fraction, while a fainter signal was detectable in Np. On the other hand, a less prominent pp65 signal was observable in the Nuc fraction in cells synchronized in S. In the latter phase, pp65 was predominant in the nucleoplasm; interestingly, a slight immunolabeling of the viral protein was detected also in the Cyt fraction. These data are in agreement with the fluorescence patterns shown in Figure 2B, and support the conclusion that, in spite of the cell-cycle-independent virus entry, the accumulation of pp65 in nucleoli is cell-cycle-dependent.

The distribution of cytoplasmic and nucleoplasmic markers confirmed the quality of the cell fractionation procedure used in the above-described experiment. Indeed, β tubulin was detected in

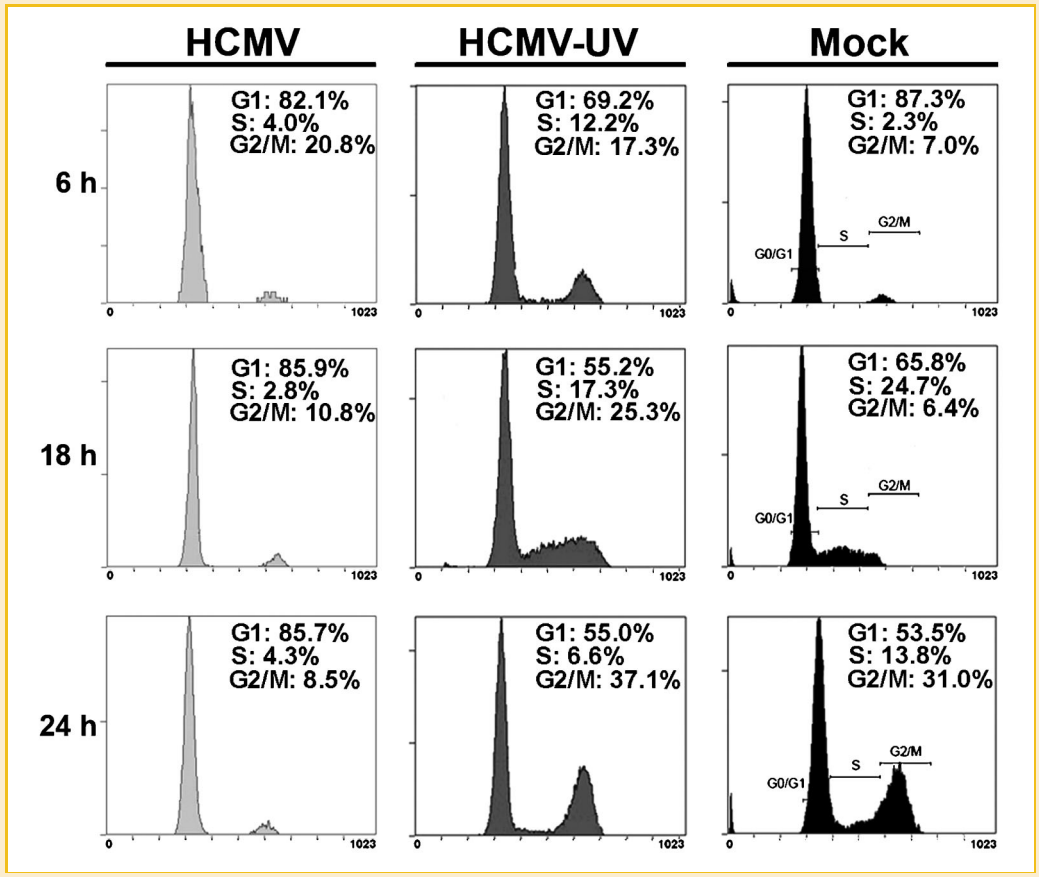

Fig. 5. Flow cytometry analysis demonstrating the suppression of the S-phase entry following HCMV infection. MRC5 confluent monolayers (G0) were subcultured in 3-cm Petri dishes, allowed to adhere to the substrate for 4 h, then infected (m.o.i. = 3) with active virus (HCMV), or UV-inactivated virus (HCMV-UV) or mock infected for 2, 14, or 20 h. This procedure allowed to monitor the cell-cycle progression after a total 6, 18, and 24 h after seeding (times corresponding to G1, S, and G2/M synchronized cells; see Fig. 1). At the indicated times, cells were harvested and stained with propidium iodide, then subjected to analysis by flow cytometry of the relative DNA amount, expressed as relative percentage of G1, S, and G2/M in the cells population.

total cellular lysate and in cytoplasmic fraction while PML protein was detected only in total cellular lysate and in nucleoplasm.

MODULATION OF HCMV GENE EXPRESSION DURING THE CELL-CYCLE PHASES IN MRC5 SYNCHRONIZED CELLS

MRC5 monolayers grown to confluence, were synchronized in G1, G1/S, S, and G2/M cell-cycle phases as described above, then infected with the HCMV AD169 strain for 3 h. Flow cytometry analysis of the DNA content and de novo expression of viral IE proteins was performed (Fig. 4A; green spots: infected cells; black spots: uninfected cells). The dot-plot graphics show that the development of infection was highly effective when cells were in G1 (55% of cells positive for IE) and/or G1/S (52%), while it was very poor in S (14%) and G2/M (19%) cell-cycle phases. It should be emphasized that we have used a very mild synchronization procedure. Thus, the samples collected at 18 and 24 h after re-seeding were enriched in S and G2/M cells, but still contained a residual portion of G1 cells. Examination of the results presented in Figure 4A makes it possible to conclude that, even in samples enriched in S and G2/M, IE-positive cells were predominantly in G1 phase.

As a further support to the cytofluorimetry data, using the same infection and synchronization conditions adopted for that experiment, IF was performed on infected cells (Fig. 4B), using antibodies directed against IE (IEp72 and IEp86) viral proteins (in green). The results confirm the data obtained by cytofluorimetry, that is, a strong IF signal prevails in G1 and G1/S, while only a small number of infected cells can be detected in S and G2/M.

In order to extend the IF results to the whole program of lytic gene expression, the patterns of viral transcripts representative of the immediate-early, early, and late phases of HCMV replication cycle were studied in synchronous cells. Monolayers of MRC5 fibroblasts were synchronized in G1 and S phases and then infected with HCMV. Total RNA was extracted after 3 or 24 h of infection. The extracted RNAs were reverse transcribed and subjected to a PCR amplification (RT-PCR) using specific primers [Ioudinkova et al., 2006] for immediate-early, early, and late proteins of HCMV. The results (Fig. 4C) show that there is a marked difference between the levels of HCMV-encoded transcripts in cells infected in G1 or S phase, with a significantly higher level of viral gene transcripts present in G1. In particular, after 3 h of infection, the expression of

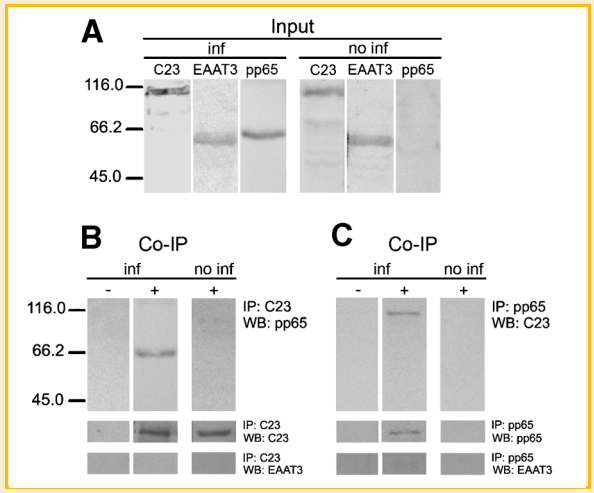

Fig. 6. Reciprocal co-immunoprecipitation (Co-IP) from infected (inf) or uninfected (no inf) cell lysates (input). MRC5 fibroblasts were mock infected or infected with HCMV AD169 strain (m.o.i. = 3), then harvested after 3 h. Panel A: WB from input samples was performed with antibodies directed against nucleolin (C23), EAAT3 (a cell membrane transporter protein), and the viral tegument phosphoprotein pp65. Panels B, C: Immunoprecipitation was done from cell lysates using either a polyclonal antibody against C23 (B) or a monoclonal antibody against pp65 (C); a pre-immune rabbit serum was used as a negative IP control. The immunoprecipitated ("+") and the mock-immunoprecipitated ("−") complexes were analyzed by WB for the presence of the viral antigen pp65 or the nucleolar protein C23 (panels B and C, respectively). The same samples were Western blotted with antibodies directed against the nucleolar protein C23 (panel B: bottom insets), the viral tegument protein pp65 (panel C: bottom insets), and EAAT3 (panels B, C: bottom insets), the latter used as a negative control (i.e., not associated with nucleolin or pp65). Molecular weight markers are indicated on the left.

IE1 was stronger in cells infected in G1 than in S phase. Expression levels of IE1 increased slightly in S-phase cells at 24 h after infection, probably due to the accumulation of the IE transcripts and to the high sensitivity of the technique used. On the other hand, a reduced expression of early and late viral transcripts (DNA polymerase, pp65, and pp150) in S, compared to G1 infected cells, was still clearly appreciable at 24 h p.i.

To find out if HCMV is able to alter the cell-cycle profile of MRC5 human embryo fibroblasts, the DNA content was monitored by flow cytometry analysis in three different conditions: mock infected, HCMV and UV-inactivated virus (HCMV-UV) infected cells (Fig. 5). HCMV infected cells did not increase the S phase percentage (i.e., were arrested in G1 or G1/S transition phases) at the considered times. On the contrary, the DNA distribution of mock or HCMV-UV infected cells shows the typical profile of the cell-cycle progression (see also Fig. 1). In another experiment we have demonstrated that HCMV infection of quiescent fibroblasts pushes the cells from G0 towards G1/S—early S, but further progression into the next phases is blocked (see Supplementary Fig. S1).

INTERACTION BETWEEN HCMV pp65 AND NUCLEOLIN

Preliminary confocal microscopy experiments on pp65 and specific nucleolar proteins release from the nucleolus (using actinomycin D at low concentration), emphasized a similar release kinetics for nucleolin (C23) and the viral protein, that were both delocalized from nucleoli very early after drug treatment (data not shown).

To evaluate whether C23 interacts with pp65 in infected cells in vitro, Co-IP experiments from uninfected (no inf) or HCMV-infected (inf) MRC5 cell lysates (input) were carried out (Fig. 6). Protein complexes were immunoprecipitated with either C23- or pp65-specific antibodies, followed by WB.

The results show that, as expected, C23 and the cell membrane transporter protein EAAT3 (a protein not associated with nucleolin or pp65) were detected in the input samples from uninfected and infected cells, while pp65 was found only in infected cells (Fig. 6A). Co-IP experiments using a polyclonal anti-C23 antibody for IP and an anti-pp65 antibody for WB (Fig. 6B), demonstrate that the viral tegument phosphoprotein (65 kDa) was co-immunoprecipitated with nucleolin (with a molecular mass of approximately 100–110 kDa, if extensively post-translationally modified).

Reciprocal Co-IP using a monoclonal antibody anti-pp65 to immunoprecipitate protein complexes from cell lysates and an antibody anti-C23 for WB (Fig. 6C), shows the presence of the nucleolar protein only in infected cells.

WB analysis of the immunoprecipitated fractions also revealed the presence of C23 in both uninfected and infected cells (Fig. 6B, bottom insets), and pp65 in infected cells (Fig. 6C, bottom insets). In control experiments, no signal was detected when an anti-EAAT3 antibody was used for staining of proteins co-immunoprecipitated with antibodies against either C23 or pp65 (Fig. 6B and C, respectively, bottom insets). Taken together, the data shown in Figure 6 demonstrate reciprocal Co-IP of pp65 and nucleolin, supporting the hypothesis of their interaction during infection.

DISCUSSION

The aim of this study was to extend our knowledge about the functional significance of the incoming HCMV pp65 accumulation within the nucleolar compartment. With this aim we have analyzed whether nucleolar localization of HCMV pp65 depends on the phase of the cell cycle.

In this regard, it should be mentioned that the events spanning the G1 to S phase transition are among the most important of the cell cycle. In particular, it is known that the retinoblastoma (Rb) family of cell protein regulators plays an important role in these early events, mediating the inhibition of transcription factors, such as members of E2F complex that are involved in the activation of genes important for committing the cell towards the S phase. Phosphorylation of Rb members in late G1 releases functional E2F allowing the cell to produce enzymes and other molecules necessary for effective DNA synthesis [Cam and Dynlacht, 2003; Hume and Kalejta, 2009]. Furthermore, in late G1 the assembly of pre-replication complexes on replication origins occurs; in particular, the loading of the mini-chromosome maintenance (MCM) complex onto proteins bound to the replication origins [Lei and Tye, 2001; Weibusch et al., 2003].

It has previously been reported that although the development of HCMV lytic infection is associated with changes in the phospho-

rylation levels of Rb proteins, higher cyclin E expression and transcriptionally active E2F (all markers of a cell entering the S phase), virus DNA synthesis does not occur in parallel with cellular DNA replication [Biswas et al., 2003]. Cytomegalovirus itself has been found to modify the normal progression of the cell cycle to its own benefit in several experimental models, mostly by blocking cycling cells in G1 and G1/S [Dittmer and Mocarsky, 1997; Fortunato et al., 2002; Hertel and Mocarski, 2004; Bain and Sinclair, 2007].

Data have been produced supporting the notion of a virus-induced blockade of the progression of the cell cycle at the G1/S border by interfering with the correct formation of competent pre-replication centers, apparently by preventing the MCM complex loading onto chromatin [Weibusch et al., 2003]. This is followed by the development of HCMV replication program. On the other hand, it has also been demonstrated that HCMV is not able to arrest cellular DNA replication when it is already in progress (i.e., when the infection occurs during S phase). In this case, the progression of HCMV replication program is postponed until the next G1 phase [Fortunato et al., 2002; Hertel and Mocarski, 2004].

It is therefore likely that HCMV could have developed a dual strategy first to alter the progression of the cell cycle with the aim of ensuring a cellular environment that supports efficient DNA synthesis, and second to highjack cellular enzymes for its own genome replication, thus abolishing cellular DNA synthesis.

The results of the present study are in agreement with the conclusions of the above-mentioned authors, showing that cells supporting an effective and complete HCMV gene expression reside almost exclusively in G1 (and G1/S), and that these cells do not progress towards the next phases of the cell cycle. On the other hand, if the host cells are already committed for cellular DNA synthesis upon viral infection (S phase), this condition does not allow the replication of viral genome, as clearly demonstrated by our data showing, in particular, the absence of the early (among them viral DNA polymerase) and late HCMV transcripts in S-phase cells.

Moreover, our results suggest that HCMV acquires control of the cell cycle by modifying and/or compromising some of the nucleolar functions. We have previously reported that the incoming HCMV tegument protein pp65 accumulates into the nucleoli during the very early stages of lytic infection and that the inability to localize pp65 to the nucleolar compartment correlates with the inhibition of HCMV immediate-early protein synthesis [Arcangeletti et al., 2003, 2009]. In the present study we have demonstrated that the nucleolar localization of pp65 of the incoming virion does not occur in S-phase cells, but that it is prominent in G1 and G1/S.

Although the main function of the nucleolus is the production of ribosomes, it has become increasingly evident that it is also involved in the regulation of cell cycle and apoptosis [Couté et al., 2006]. These ''non-canonical'' functions of nucleoli are mediated by several multi-functional nucleolar proteins. For instance, nucleophosmin was found to interact with the hyperphosphorylated form of Rb, allowing the transition into the S phase [Takemura et al., 2002]. Furthermore, the increase of rDNA transcription during G1 progression depends on the phosphorylation of the nucleolus-shuttling protein upstream-binding factor (UBF) [Sirri et al., 2008]. Depletion of another multifunctional nucleolar protein, Yph1p, which forms complexes with both origin recognition complex (ORC) proteins and ribosomal proteins, results in cycle arrest at the G1/S border [Du and Stillman, 2002]. Moreover, nucleolin, one of the major nucleolar proteins, has been described to associate with Rb during the G1 phase of the cell cycle; the deregulation of nucleolin activity, due to a loss of Rb, contributes to cellular proliferation [Grinstein et al., 2006]. Other data suggest that nucleolin may be involved in control of DNA replication under heat shock and normal conditions [Kim et al., 2005; Ugrinova et al., 2007; Greco, 2009]. It appears that reversible protein phosphorylation is the main post-translational regulatory mechanism that controls key events during the cell cycle and that it is mainly regulated by the nucleolus [Hiscox, 2007].

The Co-IP data presented in this study suggest that there is an interaction between pp65 and nucleolin during HCMV infection in vitro. Existence of such an interaction reinforces the notions stated above because of the postulated kinase activity of HCMV pp65 [Somogyi et al., 1990] and the ability of pp65 to interact with other viral and/or cellular kinases [Gallina et al., 1999; Kamil and Coen, 2007].

Thus, it is conceivable that this tegument protein might be involved in the modulation of phosphorylation events related to G1 and G1/S transition in the nucleolar compartment.

Furthermore, it is tempting to suggest that HCMV tegument protein pp65 causes delocalization, or inactivation, of one or several nucleolar proteins involved in the control of the cell cycle and thus triggers the arrest of cell-cycle progression. The inability of pp65 to accumulate into the nucleoli of dividing cells may explain the necessity of postponing the development of HCMV lytic cycle until the next G1 phase. It is therefore important to remember that pp65, which significantly accumulates into nucleoli of infected cells, is not a product of de novo viral protein synthesis, but that it enters the infected cell as a virion component. Thus, a still unknown mechanism should exist which prevents localization of this incoming HCMV protein to the nucleoli of S-phase cells. Work is in progress to answer these questions.

Gaining further insight into the interactions between HCMV and the nucleolus will facilitate a more detailed understanding of the cell biology of the nucleolus and also contribute to the design of novel anti-viral therapies.

ACKNOWLEDGMENTS

We would like to thank Prof. Ovidio Bussolati (Unit of General and Clinical Pathology, Department of Experimental Medicine, University of Parma, Italy) for generously providing the EAAC1 antibody.

REFERENCES

Ahn JH, Hawyard GS. 2000. Disruption of PML-associated nuclear bodies by IE1 correlates with efficient early stages of viral gene expression and DANN replication in human cytomegalovirus infection. Virology 274:39–55.

Arcangeletti C, Sutterlin R, Aebi U, De Conto F, Missorini S, Chezzi C, Scherrer K. 1997. Visualization of prosomes, intermediate filament and actin networks by ''instantaneous fixation'' preserving the cytoskeleton. J Struct Biol 119:35–58.

Arcangeletti MC, De Conto F, Ferraglia F, Pinardi F, Gatti R, Orlandini G, Calderaro A, Motta F, Medici MC, Valcavi P, Razin SV, Chezzi C, Dettori G. 2003. Human cytomegalovirus proteins pp65 and IEp72 are targeted to distinct compartments in nuclei and nuclear matrices of infected human embryo fibroblasts. J Cell Biochem 90:1056–1067.

Arcangeletti MC, Rodighiero I, De Conto F, Gatti R, Orlandini G, Ferraglia F, Motta F, Covan S, Razin SV, Dettori G, Chezzi C. 2009. Effect of rRNA synthesis and ppUL83 nucleolar compartmentalization on human cytomegalovirus gene expression in vitro. J Cell Biochem 108:415–423.

Bain M, Sinclair J. 2007. The S phase of the cell cycle and its perturbation by human cytomegalovirus. Rev Med Virol 17:423–434.

Biswas N, Sanchez V, Spector DH. 2003. Human cytomegalovirus infection leads to accumulation of geminin and inhibition of the licensing of cellular DNA replication. J Virol 77:2369–2376.

Boisvert FM, van Koningsbruggen S, Navascués J, Lamond AI. 2007. The multifunctional nucleolus. Nat Rev Mol Cell Biol 8:574–585.

Boyne JR, Whitehouse A. 2006. Nucleolar trafficking is essential for nuclear export of intronless herpesvirus mRNA. Proc Natl Acad Sci USA 103:15190–15195.

Callé A, Ugrinova I, Epstein AL, Bouvet P, Diaz JJ, Greco A. 2008. Nucleolin is required for an efficient herpes simplex virus type 1 infection. J Virol 82: 4762–4773.

Cam H, Dynlacht BD. 2003. Emerging roles for E2F: Beyond the G1/S transition and DNA replication. Cancer Cell 3:311–316.

Cawood R, Harrison SM, Dove BK, Reed ML, Hiscox JA. 2007. Cell cycle dependent nucleolar localization of the Coronavirus nucleocapsid protein. Cell Cycle 6:863–867.

Chang ML, Chen TH, Ming YM, Yeh CT. 2009. Cell cycle perturbation in hepatocytes of HCV core transgenic mice following common bile duct ligation is associated with enhanced p21 expression. J Med Virol 81:467–472.

Couté Y, Burgess JA, Diaz JJ, Chichester C, Lisacek F, Greco A, Sanchez JC. 2006. Deciphering the human nucleolar proteome. Mass Spectrom Rev 25:215–234.

Dittmer D, Mocarsky ES. 1997. Human cytomegalovirus infection inhibits G1/S transition. J Virol 71:1629–1634.

Du YC, Stillman B. 2002. Yph1p, an ORC-interacting protein: Potential links between cell proliferation control, DNA replication, and ribosome biogenesis. Cell 109:835–848.

Fortunato EA, Sanchez V, Yen YJ, Spector DH. 2002. Infection of cells with human cytomegalovirus during S phase results in a blockade to immediate-early gene expression that can be overcome by inhibition of the proteasome. J Virol 76:5369–5379.

Galati D, Bocchino M. 2007. New Insights on the perturbations of T cell cycle during HIV infection. Curr Med Chem 14:1920–1924.

Gallina A, Simoncini L, Garbelli S, Percivalle E, Pedrali-Noi G, Lee KS, Erikson RL, Plachter B, Gerna G, Milanesi G. 1999. Polo-like kinase 1 as a target for human cytomegalovirus pp65 lower matrix protein. J Virol 73:1468–1478.

Gobbi G, Ricci F, Malinverno C, Carubbi C, Pambianco M, Panfilis G, Vitale M, Mirandola P. 2009. Hydrogen sulfide impairs keratinocyte cell growth and adhesion inhibiting mitogen-activated protein kinase signaling. Lab Invest 89:994–1006.

Greco A. 2009. Involvement of the nucleolus in replication of human viruses. Rev Med Virol 19:201–214.

Grinstein E, Shan Y, Karawajew L, Snijders PJ, Meijer CJ, Royer HD, Wernet P. 2006. Cell cycle-controlled interaction of nucleolin with the retinoblastoma protein and cancerous cell transformation. J Biol Chem 281:22223–22235.

Hamid NA, Brown C, Gaston K. 2009. The regulation of cell proliferation by the Papillomavirus early proteins. Cell Mol Life Sci 66:1700–1717.

Hertel L, Mocarski ES. 2004. Global analysis of host cell gene expression late during cytomegalovirus infection reveals extensive dysregulation of cell cycle gene expression and induction of pseudomitosis independent of US28 function. J Virol 78:11988–12011.

Hiscox JA. 2002. The nucleolus—A gateway to viral infection? Arch Virol 147:1077–1089.

Hiscox JA. 2007. RNA viruses: Hijacking the dynamic nucleolus. Nat Rev Microbiol 5:119–127.

Hume AJ, Kalejta RF. 2009. Regulation of the retinoblastoma proteins by the human herpesviruses. Cell Div 4:1.

Ioudinkova E, Arcangeletti MC, Rynditch A, De Conto F, Motta F, Covan S, Pinardi F, Razin SV, Chezzi C. 2006. Control of human cytomegalovirus gene expression by differential histone modifications during lytic and latent infection of a monocytic cell line. Gene 384:120–128.

Ishov AM, Vladimirova OV, Maul GG. 2002. Daxx-mediated accumulation of human cytomegalovirus tegument protein pp71 at ND10 facilitates initiation of viral infection at these nuclear domains. J Virol 76:7705–7712.

Kamil JP, Coen DM. 2007. Human cytomegalovirus protein kinase UL97 forms a complex with the tegument phosphoprotein pp65. J Virol 81:10659–10668.

Kim K, Dimitrova DD, Carta KM, Saxena A, Daras M, Borowiec JA. 2005. Novel checkpoint response to genotoxic stress mediated by nucleolin-replication protein a complex formation. Mol Cell Biol 25:2463–2474.

Lee HR, Kim DJ, Lee JM, Choi CY, Ahn BY, Hawyard GS, Ahn JH. 2004. Ability of the human cytomegalovirus IE1 protein to modulate sumoylation of PML correlate with its functional activities transcriptional regulation and infectivity in cultured fibroblast cells. J Virol 78:6527–6542.

Lei M, Tye BK. 2001. Initiating DNA synthesis: From recruiting to activating the MCM complex. J Cell Sci 114:1447–1454.

Lymberopoulos MH, Pearson A. 2007. Involvement of UL24 in herpes-simplex-virus-1 induced dispersal of nucleolin. Virology 363:397–409.

Matthews DA. 2000. Adenovirus protein V induces redistribution of nucleolin and B23 from nucleolus to cytoplasm. J Virol 75:1031–1038.

Michienzi A, De Angelis FG, Bozzoni I, Rossi JJ. 2006. A nucleolar localizing Rev binding element inhibits HIV replication. AIDS Res Ther 3:13.

Muramatsu M, Onishi T. 1978. Isolation and purification of nucleoli and nucleolar chromatin from mammalian cells. Methods Cell Biol 17:141–161.

Muramatsu M, Smetana K, Busch H. 1963. Quantitative aspects of isolation of nucleoli of walker carcinosarcoma and liver of the rat. Cancer Res 23:510–518.

Pederson T, Tsai RYL. 2009. In search of nonribosomal nucleolar protein function and regulation. J Cell Biol 184:771–776.

Pliss A, Koberna K, Vecerova J, Malinsky J, Masata M, Fialova M, Raska I, Berezney R. 2005. Spatio-temporal dynamics at rDNA foci: Global switching between DNA replication and transcription. J Cell Biochem 94:554–565.

Ruggero D, Pandolfi PP. 2003. Does the ribosome translate cancer? Nat Rev Cancer 3:179–192.

Russell J, Zomerdijk JCBM. 2005. RNA-polymerase-I-directed rDNA transcription, life and works. Trends Biochem Sci 30:90–94.

Salsman J, Zimmerman N, Chen T, Domagala M, Frappier L. 2008. Genome wide screen of three herpesviruses for protein subcellular localization and alteration of PML nuclear bodies. Plos Pathog 4(7):e1000100.

Sanchez V, Angeletti PC, Engler JA, Britt WJ. 1998. Localization of human cytomegalovirus structural proteins to the nuclear matrix of infected human fibroblasts. J Virol 72:3321–3329.

Sarfraz S, Hamid S, Siddiqui A, Hussain S, Pervez S, Alexander G. 2008. Altered expression of cell cycle and apoptotic proteins in chronic hepatitis C virus infection. BMC Microbiol 8:133.

Shimakami T, Honda M, Kusakawa T, Murata T, Shimotohn K, Kaneko S, Murakami S. 2006. Effect of hepatitis C virus (HCV) NS5B-nucleolin interaction on HCV replication with HCV subgenomic replicon. J Virol 80:3332–3340.

Sirri V, Urcuqui-Inchima S, Roussel P, Hernandez-Verdun D. 2008. Nucleolus: The fascinating nuclear body. Histochem Cell Biol 129:13–31.

Somogyi T, Michelson S, Masse MG. 1990. Genomic location of a human cytomegalovirus protein with protein kinase activity (PK68). Virology 174: 276–285.

Takemura M, Ohoka F, Perpelescu M, Ogawa M, Matsushita H, Takaba T, Akiyama T, Umekawa H, Furuichi Y, Cook PR, Yoshida S. 2002. Phosphorylation-dependent migration of retinoblastoma protein into the nucleolus triggered by binding to nucleophosmin/B23. Exp Cell Res 276:233–241.

Ugrinova K, Monier K, Ivaldi C, Thiry M, Storck S, Mongelard F, Bouvet P. 2007. Inactivation of nucleolin leads to nucleolar disruption, cell cycle arrest and defects in centrosome duplication. Mol Biol 8:66–82.

Weibusch L, Uecker R, Hagemeier C. 2003. Human cytomegalovirus prevents replication licensing by inhibiting MCM loading onto chromatin. EMBO Rep 4:42–46.